

Model Based Bearing Fault Detection Using Support Vector Machines

Karthik Kappaganthu¹, C. Nataraj¹, Biswanath Samanta¹

¹ Department of Mechanical Engineering, Villanova University, Villanova, PA, 19333, USA
karthik.kappaganthu@villanova.edu
nataraj@villanova.edu
biswanath.samanta@villanova.edu

ABSTRACT

This paper deals with the development of a model based method for bearing fault diagnostics. This method effectively combines the information available in the data and the model for efficient classification of the bearing and the type of defect. A four degrees of freedom nonlinear rigid rotor model is used to simulate the rotor bearing system. Precession of the shaft is measured using proximity probes. The deviation of the measurement from the model is used to classify the system. Typically proximity probe data by itself does not contain enough information for accurate classification. However, when the information from the model is incorporated the combined features provide excellent classification performance. Further the use of a model also enables better classification over varying parameters. A support vector machine is used for classification.

1 INTRODUCTION

Rotating machinery are probably among the most important components in industry. It is important to constantly maintain these machines in proper working conditions. Ability to confidently determine the state of the system and predict failures would greatly increase the productivity of the plant. Rotating machines are composed of different sub-systems interacting with each other in a nonlinear fashion; changes in any of these components can significantly affect the overall performance. Bearings are the load bearing members of rotating machines. They are the key to effective functioning of the machine and often the cause of failure. Hence it is critical to be able to detect a faulty bearing.

Numerous techniques have been developed to analyze the vibration measurements for the purpose of diagnostics and prognostics. These techniques include extracting features and analyzing them using pattern recognition algorithms. The features can be obtained using time (Tandon, 1994), frequency (Barkova and

Barkov, 1995; Randall and Gao, 1994; Ypma, 2001) and time-frequency domain techniques (Cade *et al.*, 2005; Mori *et al.*, 1996; Ypma, 2001). For the purpose of prognosis it is necessary to track the progression of the some health indices and determine the time to failure based on this progression.

Almost all of these techniques are applied on accelerometer data measured at the bearing casing. There is little work on bearing fault detection using displacement data measured with proximity probes. This is due the fact that proximity probe data does not contain enough information about the fault. (Holm-Hansen and Gao, 2000; Yu *et al.*, 2002) are some of the few works we know that attempted to use proximity probe data for bearing fault detection. In this paper it attempted to combine the proximity probe data and a mathematical model in order to increase the usability of proximity probe data for bearing fault detection. The advantage of using proximity probe data is that there is lesser noise content in the signal. In some cases it might be more convenient to measure displacements at the shaft rather than the vibration at the bearing casing. Further the signal processing to be performed on the proximity probe data is typically lesser. Also, displacement measurements at the shaft are more direct than the vibration measurements at the bearing casing where the signal passes through the casing before being captured. However, we do not claim proximity probe data is better than accelerometer data. Accelerometer data has useful as it is rich in the frequency information which can easily capture the impulses generated by the rolling element passing through the defect (Barkova and Barkov, 1995).

Rotor-bearing models have been well developed. (Nataraj and Pietrusko, 2005; Sawalhi and Randall, 2008; Liew *et al.*, 2002) are some insightful references. The model of rotor-bearing system is a approximation of the real system, however it is an useful first step in the process of identifying the interaction between various parameters, states and features. Also models generalize the system so that efficient algorithms based on models can be applied to various systems with little modifications.

The basic idea in this paper is that the defect free model would explain the defect free system better than a system with a defect. Consider the figure shown in Figure. 1. In the figure let the triangles represent the defect free model prediction in the feature space, the

This is an open-access article distributed under the terms of the Creative Commons Attribution 3.0 United States License, which permits unrestricted use, distribution, and reproduction in any medium, provided the original author and source are credited.

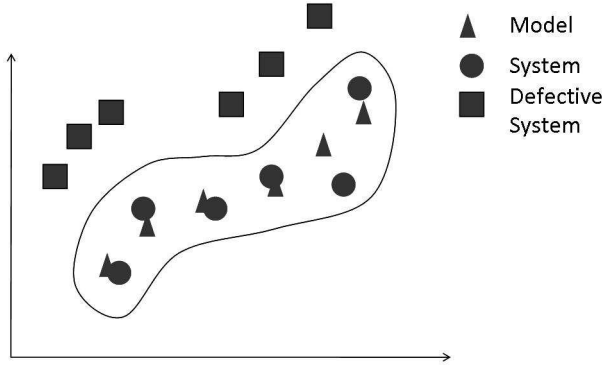


Figure 1: CLUSTERING

circles be the data from a defect free system and the squares be the data from a system with a defect. If an accurate enough model is used then the data from a defect free system would be closer to the model than the data from a system with a defect. This clustering of data can be used for effective classification of data.

The experimental setup and the data collected is discussed in the next section followed by a section on model development. Support vector machines which have good performance with lesser data (Haykin, 1999) are used for classification. They also sufficiently generalize the process; the details are explained in section 4. In section 5 the algorithm for classification is explained. The discussion on the simulations on results is presented in 6.

2 EXPERIMENTAL SETUP AND DATA COLLECTION

All the experimental data was collected on a 'Machine Fault Simulator (MFS)' (Spectra Quest, 2009) Fig. 2. It is a test rig with a rotating shaft on a two ball bearings. The speed can be controlled using a closed loop motor controller from a PC. The shaft and the motor are connected using a flexible coupling to minimize misalignment effects. The shaft is loaded using a bearing loader and balancing disks. The different parts of the system can be conveniently assembled and disassembled. The bearings are placed in the bearing casing and can easily be replaced. The bearing parameters for the system used are given in Table 1. The system was loaded with a 5 kg mass. The signals from the MFS were collected using accelerometers placed on the bearing casing; once with a defect-free bearing, once with a bearing with an outer race defect and once with a bearing with an inner race defect.

The rotating speed was varied between 1200 rpm and 2400 rpm with increments of 120 rpm. The data was captured at a sampling rate of 25 kHz and low passed filtered at frequency of twice the inner race ball pass frequency. The ball pass frequency of a bearing can be calculated from the geometry of the bearing and the rotating speed using Eq. 1. This was chosen because of all the common frequencies associated to bearing signal Ω_{bpf_i} is the highest in value, hence providing a good relevant frequency range. At each rotating speed, 10 sets of data were collected. Five of these

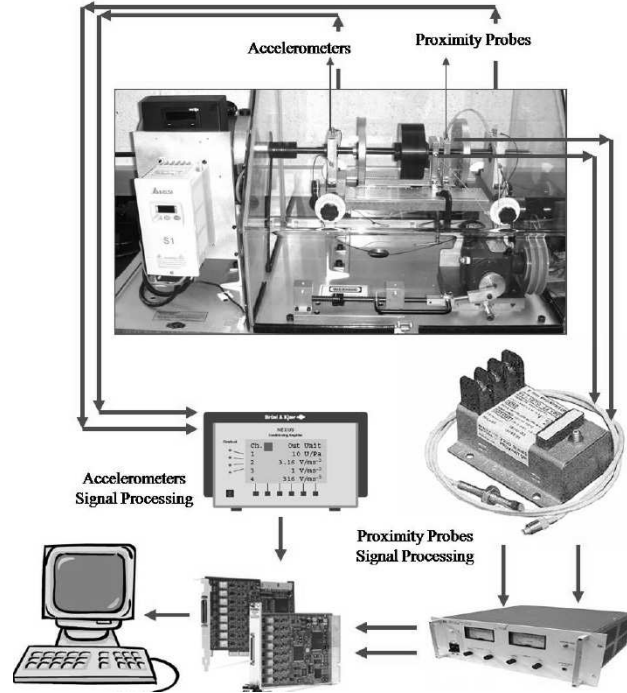


Figure 2: EXPERIMENTAL SETUP

Parameter	Value
Number of Rolling Elements (N_b)	8
Pitch Diameter (D_m)	1.319 in
Rolling Element Diameter (D_b)	.3125 in
Ball Pass Frequency Outer (Ω_{bpf_o})	3.05 Ω

Table 1: Bearing Parameters

were used in the training set and five in the test set.

$$\Omega_{bpf_i} = N_b(1 + D_b/D_m)\Omega/2 \quad (1)$$

3 ROTOR-BEARING SYSTEM MODELING

The rotor-bearing system is modeled as a rigid rotor model on nonlinear bearings. A rigid rotor model is well accepted in rotor dynamics literature. It is reasonably valid up to the first two critical speeds. The bearings are modeled using Hertzian contact forces and the outer race defects as pits. The bearing stiffness and damping are implicit in the bearing force. The rotor-bearing system and the rolling element bearing are shown schematically in Figs. 3 and 4.

The rotor-bearing system has four degrees of freedom $q = [V \ W \ B \ \Gamma]^T$. V , W are the displacement degrees of freedom and B , Γ are the angular degrees of freedom. The forces acting on the rigid rotor with mass m , inertia I_D and polar moment of inertia I_p are the bearing forces (Q_b) and the unbalance forces (Q_u). Using the Lagrangian equation, the equation of motion for the rotor-bearing system is given by Eq. (2).

$$M\ddot{q} + (D - \Omega G)\dot{q} = Q_b + Q_u. \quad (2)$$

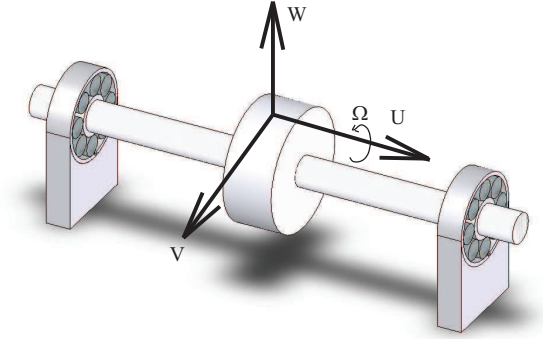


Figure 3: THE ROTOR-BEARING SYSTEM

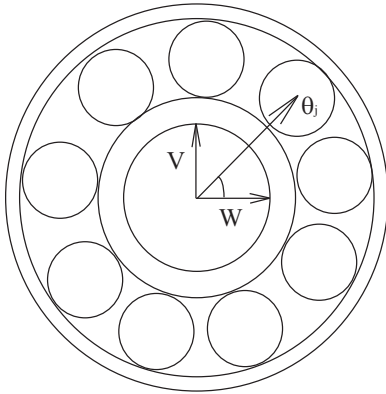


Figure 4: ROLLING ELEMENT BEARING

where M , D and G are the mass, damping and gyroscopic matrices given by Eqs. (3), (4) and (5). ρ_u and ϕ_u are the unbalance parameters of the rotor, the unbalance force Q_u is given by Eq.(9).

$$M = \begin{bmatrix} m & 0 & 0 & 0 \\ 0 & m & 0 & 0 \\ 0 & 0 & I_D & 0 \\ 0 & 0 & 0 & I_D \end{bmatrix} \quad (3)$$

$$D = \begin{bmatrix} d & 0 & 0 & 0 \\ 0 & d & 0 & 0 \\ 0 & 0 & 0 & 0 \\ 0 & 0 & 0 & 0 \end{bmatrix} \quad (4)$$

$$G = \begin{bmatrix} 0 & 0 & 0 & 0 \\ 0 & 0 & 0 & 0 \\ 0 & 0 & 0 & -I_p \\ 0 & 0 & I_p & 0 \end{bmatrix} \quad (5)$$

$$\rho_{uy} = \rho_u \cos(\phi_u) \quad (7)$$

$$\rho_{uz} = \rho_u \sin(\phi_u) \quad (8)$$

$$Q_u = m\Omega^2 \begin{bmatrix} \rho_{uy} \\ \rho_{uz} \\ 0 \\ 0 \end{bmatrix} + \Omega^2 \begin{bmatrix} -\rho_{uz} \\ \rho_{uy} \\ 0 \\ 0 \end{bmatrix} \quad (9)$$

In order to determine the bearing load on the rotor each bearing force is transferred from the bearing position to the center of mass of the rotor and summed as shown in Eq.(10).

$$Q_b = \sum_{i=1}^{N_b} A_{bi}^T Q_{bi} \quad (10)$$

A_{bi} is the transformation matrix of the bearing at a_i from the center of mass as shown in Eq. (11). Q_{bi} is the bearing force vector as shown in Eq.(12).

$$A_{bi} = \begin{bmatrix} 1 & 0 & 0 & -a_i \\ 0 & 1 & a_i & 0 \end{bmatrix} \quad (11)$$

$$Q_{bi} = [F_{xi} \ F_{yi}]^T \quad (12)$$

F_{xi} , F_{yi} are the x and y components of force exerted by i^{th} bearing on the rotor. These forces are the resultants of the nonlinear force exerted by each rolling element. The force exerted by a rolling element in load zone is obtained from Hertzian contact stress (Harris, 2002). For a rolling element bearing with N_b rolling elements, the force exerted by the j^{th} rolling element Q_j is given by Eq. (13).

$$Q_j = K_p \delta_j^n \quad (13)$$

K_p is the effective stiffness of the bearing, δ_j is the deflection of the j^{th} rolling element and n is a constant dependent on the type of the bearing. For ball bearings n is 1.5. The effective stiffness of the bearing can be calculated from the geometry (Harris, 2002) and is given by Eq. (14).

$$K_p = \left[\left(\frac{1}{K_i} \right)^{1/n} + \left(\frac{1}{K_o} \right)^{1/n} \right]^{-n} \quad (14)$$

Where K_i , K_o are the inner and outer race stiffness. For steel balls and races they are given by Eq.(15) (Harris, 2002).

$$K_{i,o} = 2.15 \times 10^5 \left(\sum \rho_{i,o} \right)^{-1/2} (\delta_{i,o}^*)^{-3/2} \quad (15)$$

$\sum \rho$ is the sum of the curvatures and $\delta_{i,o}^*$ is a function of ρ that can be determined by interpolation from standard references such as (Harsha *et al.*, 2004; Harris, 2002). Thus if θ_j is the angular position of j^{th} rolling element the force exerted by the i^{th} bearing on the shaft is given by Eq. (16)

$$Q_{bi} = \begin{bmatrix} \sum_{j=1}^{Nb} K_p \gamma_j \delta_j^n \cos(\theta_j) \\ \sum_{j=1}^{Nb} K_p \gamma_j \delta_j^n \sin(\theta_j) \end{bmatrix} \quad (16)$$

Where γ_j given by Eq.(17) is a constant to determine if the rolling element is in the load zone.

$$\gamma_j = \begin{cases} 0 & \delta_j < 0 \\ 1 & \delta_j > 0 \end{cases} \quad (17)$$

As modeled in (Nataraj and Pietrusko, 2005; Sawalhi and Randall, 2008; Liew *et al.*, 2002), the deflection of the j^{th} rolling element is a function of shaft displacement. It is shown in Eq.(18).

$$\delta_j = v \cos(\theta_j) + w \sin(\theta_j) - c \quad (18)$$

4 SUPPORT VECTOR MACHINES

Support vector machines are statistical learning theory based supervised learning machines. These are feed-forward linear learning machines and were pioneered by Vapnik (Vapnik, 1998). Support vector machines are approximate implementations of the principle of structural risk minimization. These machines provide good generalization performance on pattern classification (Haykin, 1999).

A brief overview of support vector machines is provided in this section. More detailed analysis can be found in (Haykin, 1999; Shawe-Taylor and Christianini, 2004). As a simple case consider linearly separable two dimensional data as shown in Fig. 5. Any plane in the space is given by Eq. 19. w is the weight vector, x is a point in the feature space and b is the bias vector. If data in the first class are associated with a label $d = +1$ and the data in the second class with $d = -1$ then the division of data by the hyperplane is given by Eq. 20.

$$w^T x + b = 0 \quad (19)$$

$$\begin{aligned} w^T x_i + b &\geq 0 \text{ for } d_i = +1 \\ w^T x_i + b &< 0 \text{ for } d_i = -1 \end{aligned} \quad (20)$$

For a given w and b the separation between the hyperplane and the closest data point is called the margin. The goal of the support vector machine is to maximize the margin of separation. The points which lie closest to the separating hyperplane and hence are most difficult to classify are called the support vectors. At these points Eq. 21 is satisfied. The margin of separation is inversely proportional to the norm of the weight vector. Based on the above discussion the primal optimal

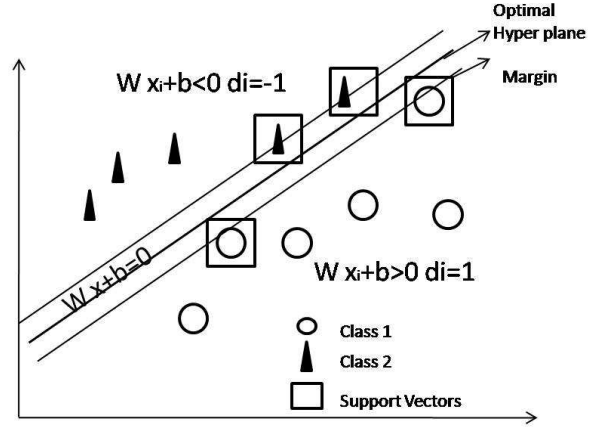


Figure 5: SUPPORT VECTOR MACHINE

problem can be defined for solving for the optimal hyperplane.

$$\begin{aligned} w^T x_i + b &= 1 \text{ for } d_i = +1 \\ w^T x_i + b &= -1 \text{ for } d_i = -1 \end{aligned} \quad (21)$$

Given training data,

$$\min \Phi(w) = \frac{1}{2} w^T w \quad (22)$$

$$d_i(w^T x_i + b) \geq 1 \text{ for } i = 1, 2, N \quad (23)$$

The above convex problem can be solved using N Lagrangian multipliers α_i and KKT conditions. However for easy execution, a dual problem can be developed which has the same solution as Eq. 22. This is given in Eq. 24.

$$Q(\alpha) = \sum_{i=1}^N \alpha_i - \frac{1}{2} \sum_{i=1}^N \sum_{j=1}^N \alpha_i \alpha_j d_i d_j x_i^T x_j \quad (24)$$

such that

$$\sum_{i=1}^N \alpha_i d_i = 0 \quad (25)$$

$$\alpha_i \geq 0 \quad (26)$$

For nonlinearly separable patterns the data is mapped into a high-dimensional feature space using a kernel K . The cost function now is given by Eq. 27.

$$Q(\alpha) = \sum_{i=1}^N \alpha_i - \frac{1}{2} \sum_{i=1}^N \sum_{j=1}^N \alpha_i \alpha_j d_i d_j K(x_i, x_j) \quad (27)$$

This can be solved using any of the popular optimization methods.

5 ALGORITHM

In this section an algorithm is developed for bearing fault identification using the data, model and support

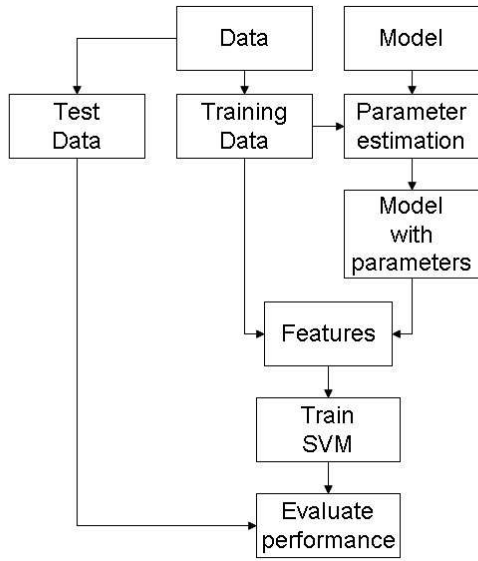


Figure 6: ALGORITHM

vector machines explained in the previous sections. The algorithm is shown in Fig. 6.

Bearing fault detection is treated as a classification problem. The three classes here are defect free system, system with inner race defect and system with an outer race defect.

The first step of the process is data collection. Data is collected at various speeds as explained earlier. The data is divided into a test set and a training set.

Since the data is collected at various speeds Ω is a varying parameter in the model. Also, each time the machine is disassembled and assembled (for changing the bearings) the unbalance parameters change. It is essential that each time right parameters are used for simulation. This is the next step in the method. Training data and least squares method are used for estimating unbalance parameters in each case.

Now, the difference between the measurement and the corresponding model for one rotation is evaluated. This is called the residue. Variance, skewness and kurtosis of the residue are used as features. The mean square error between the model and measurement is also used as a feature.

Next, the features are used to train the support vector machine. A gaussian kernel is used in the support vector machine. The test set is used for evaluating the performance of the method.

6 SIMULATION AND RESULTS

As the first step in the algorithm the data collected from the experiment is used to estimate the unknown parameters in the model developed in section 2. Unbalance magnitude and unbalance angular position are the unknowns in the system. Least-squares method is used to estimate these parameters. The error is the difference between the model and the data

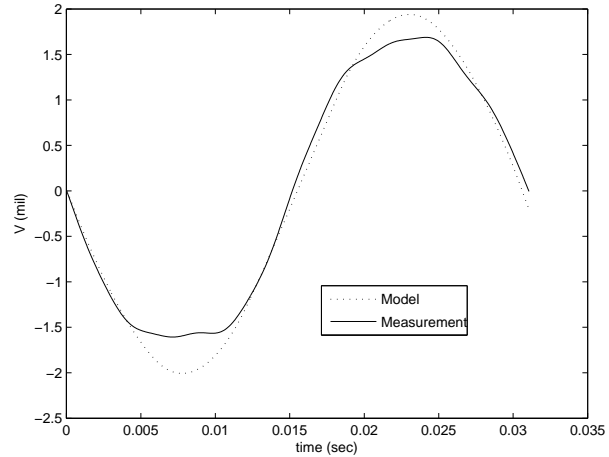


Figure 7: DEFECT FREE BEARING

over all speeds for one rotation. Mathematically this is given by Eq. 28.

$$f(\rho_u, \phi_u) = \sum_{i=1}^{N_s} \frac{1}{N_i} [R_i(\rho_u, \phi_u)]^2 \quad (28)$$

where N_s is the number of rotating speeds over which the data is collected and N_i are the number of data points in the signal at a particular rotating speed. R_i is the residue of the signal given by Eq. 29, where V_{d_i} , V_{m_i} are the data and simulation for one rotation respectively.

$$R_i = V_{d_i} - V_{m_i}(\rho_u, \phi_u) \quad (29)$$

Using the unbalance parameter obtained, the model is simulated. Figures 7, 8, and 9 show the comparison between the model and simulation for a defect free system, a system with an outer race defect and a system with an inner race defect respectively.

From the figures it can be seen that the measured signal in the system with outer race defect deviates more from the simulation when compared to the other two signals. The inner race defect signal and defect free signal are closer to each other. In fact the least square algorithm converged faster in these cases.

To exploit this observation the SVM was applied in two steps. In the first step the classification was performed as a system with and without an outer race defect. In the second step the data without an outer race defect was classified as defect free or otherwise. Variance, skewness and kurtosis of the residue were used as features. A zero mean gaussian kernel with a variance of 0.9 was used for the SVM. The upper bound for the lagrangian constants was 10^9 . Figure 10 shows the performance of the SVM. In this figure x-coordinate is the sample number and the y-coordinate is the label associated with each class. There are five samples at each speed. The defect free samples are labeled 1, the outer race defect samples are labeled 2 and the inner race defect samples are labeled 3. The upper subplot is the performance on the training set

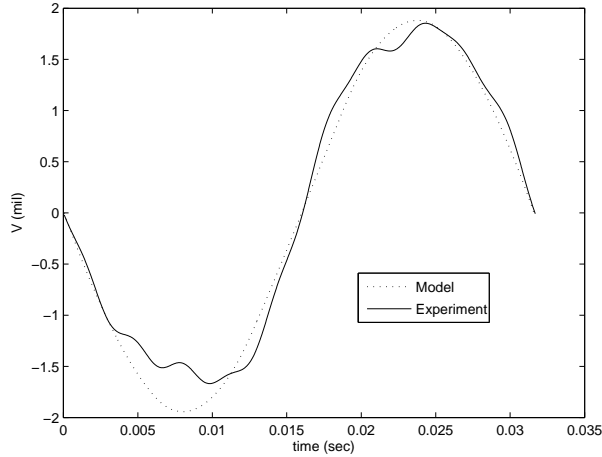


Figure 8: BEARING WITH OUTER RACE DEFECT

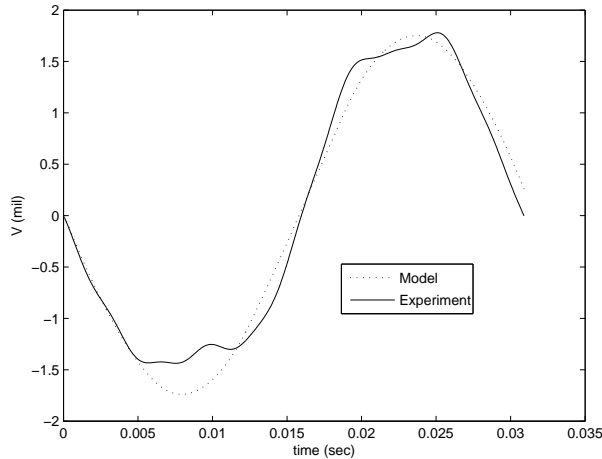


Figure 9: BEARING WITH INNER RACE DEFECT

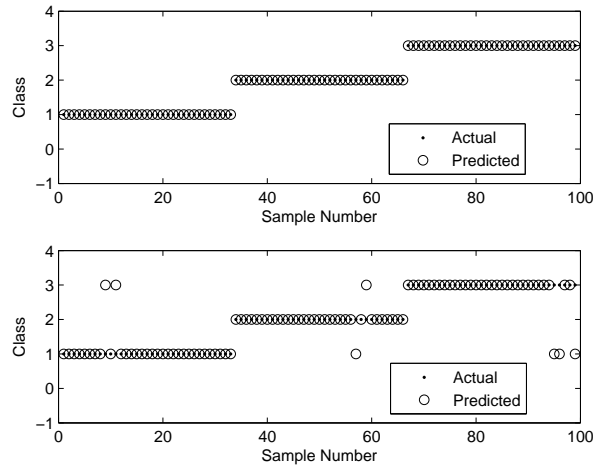


Figure 10: CLASSIFICATION PERFORMANCE WITH RESIDUAL FEATURES

	DF	ORD	IRD
DF	31	0	2
ORD	1	31	1
IRD	3	0	30

Table 2: CONFIDENCE MATRIX: RESIDUAL FEATURES

and the lower is the test set performance. There was 100 percent training success. The confidence matrix of the classification is shown Table. 2.

There were 99 observations in the test set and 99 in the training set. Both training and test sets had equal distribution of all the three classes. SVM correctly classified defect free system 31 of the 33 times. In the other two cases it classified the system as an inner race defect. SVM performed similarly in classifying the system with outer race defect. The performance was slightly less classifying inner race defect. The first stage SVM (2 misclassifications from 99 samples) performed better than the second stage SVM (4 misclassifications from 66 samples). In should be noted that the system was never misclassified as outer race defect.

In order to compare the performance of residual features, a classification based on the time domain features of the signal is also performed. In this case too variance, skewness and kurtosis were used as features. The output of this classification is shown in Fig. 11 and corresponding confidence table is shown in Table. 3. There were 99 samples in this case too and the distribution was similar to the previous case. There was 100 percent training success in this case too. But the performance of classification was degraded on the test set. There were 12 misclassifications in all. In this case there were more number of instances when the system was misclassified as an outer race defect.

7 CONCLUSION AND FUTURE WORK

In this paper nonlinear model based features were used for detecting inner race and outer race faults in a rotor

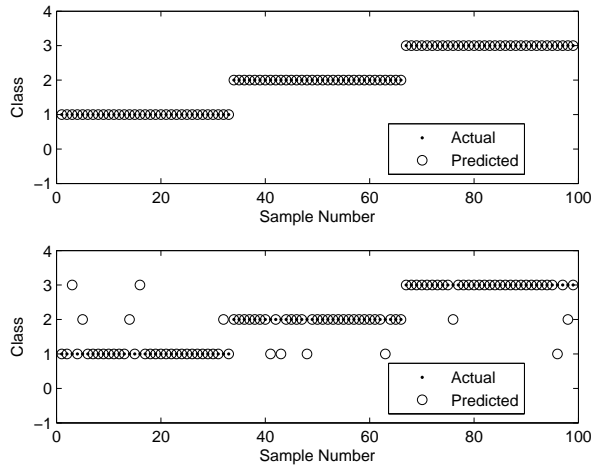


Figure 11: CLASSIFICATION PERFORMANCE WITH SIGNAL FEATURES

	DF	ORD	IRD
DF	28	3	2
ORD	4	29	0
IRD	1	2	30

Table 3: CONFIDENCE MATRIX: SIGNAL FEATURES

bearing system. Proximity probes data which typically has poor performance for bearing fault detection was augmented with information from a nonlinear model to obtain better performance. A support vector machine was used for pattern classification. The model based features performed better than just signal based features. The outer race defect system deviated more from the model than the inner race defect system and hence easier to classify. The model based features performed better in classifying outer race defects than inner race defects. The signal based features performed similarly on all three classes.

This work is just an initial study in the advantages and feasibility of using model based features. Only simple time domain features have been used in this study. More complicated features need to be developed for further study. The information in the model based features needs to be studied and compared with signal features and their performance together needs to be evaluated. More complicated models for systems with defects are being developed and time frequency domain features are being looked at. Model based features are also being studied for fault monitoring and prognostics.

ACKNOWLEDGEMENTS

This project was sponsored by Office of Naval Research (monitor: Mr. Marc Steinberg), which we would like to gratefully acknowledge. Thanks are also due to Mr. John Metzger of Naval Sea Systems Command, Philadelphia.

NOMENCLATURE

q	Degree of freedom vector
m	Mass of rotor
d	Damping coefficient
I_D	Inertia of the rotor
I_p	Polar moment of inertia of the rotor
I_p	Polar moment of inertia of the rotor
ρ_u	Unbalance magnitude
ϕ_u	Unbalance angle
N_b	Number of rolling elements in a bearing
θ_j	Angular position of the j^{th} rolling element
δ_j	Deflection at the j^{th} rolling element
K_p	Effective bearing stiffness

REFERENCES

- (Barkova and Barkov, 1995) A. Barkova and N. Barkov. Condition assesment and life prediction of rolling element bearings. *Sound and Vibration*, 1995.
- (Cade *et al.*, 2005) Iain S. Cade, Patrick S. Keogh, and M. Necip Sahinkaya. Fault identification in rotor/ magnetic bearing systems using discrete time wavelet coefficients. *IEEE/ ASME Transactions on Mechatronics*, 10(6):648–657, December 2005.
- (Harris, 2002) Tedric A. Harris. *Rolling Bearing Analysis*. Wiley-Interscience, 2002.
- (Harsha *et al.*, 2004) S. P. Harsha, K. Sandeep, and R. Prakash. Nonlinear behaviors of rolling element bearings due to surface waviness. *Journal of Sound and Vibration*, 272:557–580, 2004.
- (Haykin, 1999) Simon Haykin. *Neural Networks: A comprehensive foundation*. Prentice Hall, 1999.
- (Holm-Hansen and Gao, 2000) B. T. Holm-Hansen and R. X. Gao. Vibration analysis of a sensor-integrated ball bearing. *ASME Journal of Vibration and Acoustics*, 122:384392, 2000.
- (Liew *et al.*, 2002) A. Liew, N. Feng, and E. J. Hahn. Transient rotordynamic modeling of rolling element bearing systems. *Transactions of ASME*, 124:984–991, October 2002.
- (Mori *et al.*, 1996) K. Mori, N. Kasashmi, T. Yoshioka, and Y. Ueno. Prediction of spalling on ball bearings by applying discrete wavelet transform to vibration signals. *Wear*, 8:195–162, 1996.
- (Nataraj and Pietrusko, 2005) C. Nataraj and Robert Gerad Pietrusko. Dynamic response of rigid rotors supported on rolling element bearings with an outer raceway defect. In ASME, editor, *Proceedings of IDETC/CIE 2005*, Long Beach California, USA, September 2005.
- (Randall and Gao, 1994) R. B. Randall and Y. Gao. Extraction of modal parameters from the response of power cepstrum. *Journal of Sound and Vibration*, 176:179–193, 1994.
- (Sawalhi and Randall, 2008) N. Sawalhi and R. B. Randall. Simulating gear and bearing interactions in the presence of faults part1. the combined gear bearing model and simulation of localized bearing faults. *Mechanical Systems and Signal Processing*, 2008.

- (Shawe-Taylor and Christianini, 2004) John Shawe-Taylor and Nello Christianini. *Kernel Methods for Pattern Analysis*. Cambridge University Press, 2004.
- (Spectra Quest, 2009) Inc Spectra Quest. Http: www.spectraquest.com, 2009.
- (Tandon, 1994) N. Tandon. A comparison of some vibration parameters for condition monitoring of rolling element bearings. *Measurement*, 12:285–286, 1994.
- (Vapnik, 1998) V. N. Vapnik. *Statistical Learning Theory*. John Wiley & Sons, 1998.
- (Ypma, 2001) A. Ypma. *Learning Methods of Machine Vibration Analysis and Health Monitoring*. PhD thesis, Delft University, 2001.
- (Yu *et al.*, 2002) J. J. Yu, D. E. Bently, P. Goldman, K. P. Dayton, and B. G. Van Slyke. Rolling element bearing defect detection and diagnostics using displacement transducers. *Journal of Engineering for Gas Turbines and Power*, 124:517–527, 2002.

Karthik Kappaganthu received his Bachelors degree in Mechanical Engineering from Kakatiya University, India, and his M.S. degree in Mechanical Engineering from Villanova University, in 2004 and 2006, respectively. He is currently pursuing Ph.D in Engineering at Villanova University.

C. Nataraj received his B.S. degree in Mechanical Engineering from Indian Institute of Technology, and his M.S. and Ph.D. degrees from Arizona State University. He is currently a Professor and the Chair of the department of Mechanical Engineering at Villanova University. He is the founder and former Director of the Center for Nonlinear Dynamics & Control, an interdisciplinary research center. His research interests are in modeling, dynamics and control of nonlinear systems.

B. Samanta received B.Tech. (Honors) and Ph.D. in Mechanical Engineering from Indian Institute of Technology (IIT), Kharagpur. He is currently in the Department of Mechanical Engineering at Villanova University, Villanova, PA. Prior to joining Villanova, he held academic positions at Sultan Qaboos University, Oman and IIT, Kharagpur. His major research interests include broad areas of system dynamics and control, advanced signal processing, prognostics and health management, and applications of computational intelligence in engineering and biomedicine. He has over ninety refereed research articles published by professional bodies like ASME, IMechE, AIAA and IEEE. He is a member of ASME, ASNE, a senior member of IEEE, IEEE Computational Intelligence Society (CIS), and IEEE Engineering in Medicine and Biology Society (EMBS).